Compensation of Current Transformers' Non-Linearities by Means of Frequency Coupling Matrices

A. J. Collin, *Member, IEEE*, A. Delle Femine, *Member, IEEE*, D. Gallo, *Member, IEEE*, R. Langella , *Senior Member IEEE*, M. Luiso , *Member, IEEE*

University of Campania "Luigi Vanvitelli", Aversa (CE), Italy (adam.collin@ieee.org; antonio.dellefemine@unicampania.it; daniele.gallo@unicampania.it; roberto.langella@unicampania.it; mario.luiso@unicampania.it)

***Abstract*— Current transformers (CTs) are the most commonly installed current transducers in power systems, at all voltage levels. Therefore, the measurement of harmonics, and power quality in general, which is an essential task in the new context of Smart Grids, are strongly influenced by the performance of CTs. It is well known that CTs can exhibit a non-linear response and, therefore, in order to accurately measure harmonics with CTs, suitable non-linear mathematical models have to be used. In this paper the complex ratio of the CT is modelled using a frequency domain model based on frequency coupling matrices. An accurate measurement setup has been built to characterize the CTs performance in distorted conditions. Some preliminary results of the proposed compensation technique are presented and discussed for a commercial CT of accuracy Class 0.5.**

***Index Terms* —Current Transformer, Power System Measurement, Frequency Coupling Matrix, Harmonics, Phase-Dependent Characteristics, Power Quality.**

I. INTRODUCTION

The measurement of harmonics, and power quality in general, is an essential task, particularly in the new context of Smart Grids with a high penetration of non-linear loads and energy production from renewable sources. Nowadays, voltage and current instrument transformers (VTs and CTs) are still the most commonly installed voltage and current transducers in power systems, at all voltage levels. As a consequence, most measuring instruments for power system applications (power/energy measurement, power quality measurement, Phasor Measurement Unit, etc.) use VTs and CTs ([1]-[8]).

Some recent scientific literature ([9]-[13]) has experimentally demonstrated that even high accuracy class CTs and VTs (i.e. accuracy class better than 0.5) may suffer from non-linearity effects. Due to these effects, the accuracy of the CT/VT is strongly dependent on the amplitude, phase angle and order of harmonic content of the input waveform. Therefore, the measurement of harmonics by VTs and CTs could present an accuracy which is much lower than the accuracy class of the instrument transformer used in the measurement chain. Accordingly, an accurate harmonic measurement by a VT or CT requires the use of a non-linear mathematical (either analytic or numerical) model for the instrument transformer, which is able to accurately reconstruct the primary quantity (i.e. voltage for VTs and current for CTs) from the measured secondary quantity.

Different techniques to mathematically describe the non-linearity of instrument transformers have been proposed in scientific literature, e.g. [14]-[16]. They are essentially based on modelling the saturation and eddy currents phenomena in transformers. However, the performances of the proposed techniques have not been verified when harmonic distortion is present in the primary quantity.

Another approach to model non-linear devices, commonly used for power system harmonic penetration studies in the frequency domain, is the Frequency Coupling Matrix (FCM) approach [17]-[27]. FCMs are based on the theory of small signal analysis and here used to relate the generic harmonic component of the secondary current to the variations of all of the considered harmonic components of the primary current. They are a powerful tool able to model the non-linearities in power system components and both traditional devices (i.e. power transformers, AC motors, cables and so on) and modern devices based on power electronic technologies. FCMs can be obtained both analytically or by numerical or experimental tests.

In this paper, the FCM approach is applied to model the complex ratio of a Class 0.5 CT. First of all, the CT is accurately characterized in the presence of harmonic distortion, using the method described in [28] and [29]. Then the FCM is derived and it is shown that by inverting this matrix, the harmonic content of the primary current can be accurately identified from the measurement of the secondary current.

The paper is organized as follows. Section II gives a brief recall of the FCM approach. Section III presents the experimental setup and describes the experimental tests performed to characterize the CT. Section IV shows the derivation of the FCM of the CT under study and discusses the use of the proposed compensation technique in a practical case, i.e. the measurement of the current of a non-linear load. Conclusions are given in Section V.

II. CT COMPENSATION TECHNIQUE

Under the hypothesis of time periodic signals, the secondary current of a current transformer $i^s(t)$ is a function of the primary current, $i^p(t)$:

$$i^s(t) = g\left(i^p(t)\right), \tag{1}$$

where: g is a function which accounts for the non-linearities related to the non-ideal operation of the CT itself.

Under small-signal operation, any device can be linearized around proper operation base points $i_b^s(t)$ and $i_b^p(t)$. Evaluating the complex Fourier series of the quantities involved gives:

$$\left[\Delta \underline{\boldsymbol{I}}^s\right] = \left[\underline{\boldsymbol{I}}^s - \underline{\boldsymbol{I}}_b^s\right] = \left[\underline{\boldsymbol{G}}\right]\left[\underline{\boldsymbol{I}}^p - \underline{\boldsymbol{I}}_b^p\right] = \left[\underline{\boldsymbol{G}}\right]\left[\Delta \underline{\boldsymbol{I}}^p\right] \tag{2}$$

where: $\Delta\underline{\boldsymbol{I}}^s$ and $\Delta\underline{\boldsymbol{I}}^p$ are vectors of harmonic phasors and the function $\underline{\boldsymbol{G}}$ is a complex vector function.

If $\underline{\boldsymbol{G}}$ is linear, it may include linear cross-coupling and phase dependence between harmonics [17]. However, when linearizing general nonlinear devices, representation by a single complex number is not possible. The general representation is:

$$\Delta \underline{\boldsymbol{I}}^s = \underline{G}^{+}\Delta \underline{\boldsymbol{I}}^p + \underline{G}^{-}\Delta \underline{\boldsymbol{I}}^{p*} \tag{3}$$

where: $\underline{\boldsymbol{G}}^{+}$ and $\underline{\boldsymbol{G}}^{-}$ are two matrices of complex numbers that couple $\Delta\underline{\boldsymbol{I}}^p$ and its conjugate $\Delta\underline{\boldsymbol{I}}^{p*}$, respectively, to give $\Delta\underline{\boldsymbol{I}}^s$.

Equation (3) can be elegantly and efficiently rewritten using a real valued rank 2 tensor representation as in (4):

$$\begin{bmatrix} \begin{bmatrix} \Delta I^s_{1r} \\ \Delta I^s_{1i} \end{bmatrix} \\ \vdots \\ \begin{bmatrix} \Delta I^s_{Hr} \\ \Delta I^s_{Hi} \end{bmatrix} \end{bmatrix} = \begin{bmatrix} \begin{bmatrix} \boldsymbol{g_{1r1r}} & g_{1r1i} \\ g_{1i1r} & \boldsymbol{g_{1i1i}} \end{bmatrix} & \cdots & \begin{bmatrix} g_{1rKr} & g_{1rKi} \\ g_{1iKr} & g_{1iKi} \end{bmatrix} \\ \vdots & \ddots & \vdots \\ \begin{bmatrix} g_{Hr1r} & g_{Hr1i} \\ g_{Hi1r} & g_{Hi1i} \end{bmatrix} & \cdots & \begin{bmatrix} \boldsymbol{g_{HrKr}} & g_{HrKi} \\ g_{HiKr} & \boldsymbol{g_{HiKi}} \end{bmatrix} \end{bmatrix} \cdot \begin{bmatrix} \begin{bmatrix} \Delta I^p_{1r} \\ \Delta I^p_{1i} \end{bmatrix} \\ \vdots \\ \begin{bmatrix} \Delta I^p_{Kr} \\ \Delta I^p_{Ki} \end{bmatrix} \end{bmatrix} \tag{4}$$

where: the elements of the main diagonal, highlighted using bold characters, link the real r and imaginary i parts of the primary and secondary currents of the same harmonic order.

Equation (3) can now be written in a more compact form as follows:

$$\left[\Delta \underline{\boldsymbol{I}}^s\right] = \left[\underline{G}^{(2)}\right]\left[\Delta \underline{\boldsymbol{I}}^p\right] \tag{5}$$

If $\underline{G}^{(2)}$ is invertible, the following relation can be written:

$$\left[\Delta \underline{\boldsymbol{I}}^p\right] = \left[\underline{G}^{(2)}\right]^{-1}\left[\Delta \underline{\boldsymbol{I}}^s\right] = \left[\underline{R}^{(2)}\right]\left[\Delta \underline{\boldsymbol{I}}^s\right] \tag{6}$$

The ratio compensation matrix $\underline{R}^{(2)}$ in (6) can be used to compensate the measured secondary current spectrum.

III. EXPERIMENTAL CHARACTERIZATION OF THE CURRENT TRANSFORMER

A. Measurement setup

The block diagram of the setup for CT characterization is shown in Figure 1. Current generation is obtained through the Fluke 52120A transconductance amplifier (up to three in parallel, each one rated up to 120A, up to 10kHz).

It is driven by the National Instrument PXI 5421 arbitrary waveform generator (AWG), (± 12 V, 100 MHz maximum sampling rate, 16 bit, onboard memory 256 MB). The current reference value is obtained by means of two calibrated current shunts, LEM NORMA TRIAX Shunt: 30 / 300 A/mV (0.03 % up to 100 kHz) and 100 / 100 A/mV (0.15 % up to 100 kHz).

A versatile comparator, which can be employed for the calibration of conventional and non-conventional instrument transformers, is used to compare the outputs of the CT and the reference shunt.

Its sampling clock can be synchronized to the generation sampling clock, by exporting a 12.8 MHz signal from the AWG to the comparator.

According to the type of the test, different input channels can be used (± 7.5 A, ± 75 A, ± 500 mV, ± 10 V). Further details of the comparator are available in [28].

The amplifier and the comparator are remotely controlled, respectively through IEEE 488.2 and Ethernet, by a PXI controller running the calibration software, developed in LabVIEW.

B. CT testing procedure

In order to characterize the CT performance in the presence of distorted signals, an event based state machine has been developed in LabVIEW.

A large choice of signal types may be selected, for example: sinusoidal (SIN), fundamental plus a harmonic tone (FH1), fundamental with N harmonics (FHN), fundamental with an inter-harmonic (FI1) and so on.

All of the waveform parameters are fully controlled by the user and parameters sweeps are also possible, resulting in wide variety of possible waveforms for CT characterization.

The CT complex frequency response is determined at every frequency component that is generated.

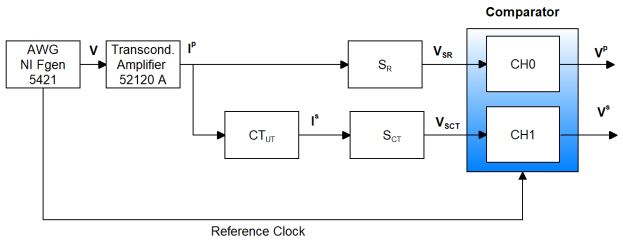

Figure 1. Block diagram of the measurement setup for CT characterization.

Depending on the sampling method, i.e. synchronous or asynchronous, the phasors of primary and secondary currents are obtained by means of Discrete Fourier Transform (DFT) or Interpolated DFT (IpDFT) [30]-[32], respectively.

However, the system is programmed in such a way that the waveforms can be stored for further post-processing, if required.

Following the calculation of all complex phasors, the ratio error (in per cent) and phase error (in crad), defined in (7) and (8), are evaluated for each frequency component of order j:

$$\Delta R_j = \left(\frac{\hat{I}_j^s}{\hat{I}_j^p} - 1 \right) \cdot 100 \tag{7}$$

$$\Delta \varphi_j = \hat{\varphi}_j^s - \hat{\varphi}_j^p \tag{8}$$

where: $\hat{I}_j^s$ ($\hat{I}_j^p$) and $\widehat{\varphi^s}_j$ ($\widehat{\varphi^p}_j$) are the estimated amplitude and phase angle of the output of the device under test (reference shunt).

C. Test description

The previously described system has been used to characterize the behaviour of a commercial, window type 500 / 5 A / A CT, with rated ratio of 100, accuracy class of 0.5, rated burden of 2.5 VA and operating frequency of 50/60 Hz.

For window-type CTs, additional primary turns can be used in order to increase the equivalent measured primary current. For the case at hand, 29 additional turns have been realized on the primary side and the 30 A reference shunt has been used. This was made in order to assimilate the CT performance obtained with 29 turns and 17.25 A to those obtainable with just one turn and 500 A.

The 29 cables were wound in a compact group and the diameter of each turn was very large with respect to the CT window area diameter, thus obtaining very similar magnetic effects to those of a 500 A current flowing in a straight single cable perpendicular to the CT core section.

The CT output current has been directly acquired with the comparator: its current terminals have an input impedance of about 12 mΩ, which corresponds to a burden of about 12 %.

A fundamental tone with 50 Hz and 0 degree phase angle plus a single harmonic tone have been used. The harmonic parameter sweep was configured with: three amplitudes (1 %, 5 % and 10 %), thirteen frequencies (from 2nd to 14th order) and thirteen phase angles (from -180 degrees to 180 degrees). For each test waveform, a sampling frequency of 10 kHz was used and 10,000 points acquired (i.e. 1s). Measurements with each test waveform were repeated ten times.

IV. Experimental Results

In this section, the proposed compensation strategy is verified. This process begins with the derivation of the ratio compensation matrix $\underline{\underline{R}}^{(2)}$ (6), which is compared against measurements of single tone (FH1) signals.

Waveforms with a fundamental component corresponding to 50% and 100% of rated, 8.625 A and 17.25 A, have been used.

An experimental case study using a synthetic waveform, which mimics the current absorption of a generic non linear load characterized by the presence of more than one harmonic, has also been conducted to further assess the performance of the derived compensation matrix.

Reference is made to the group of tests corresponding to the superimposition of the harmonic component with the amplitude of 10%. Both single iterations of each test and the averaged results obtained from the 10 repetitions have been used.

A. Compenasation Matrix Derivation

Fig. 2 shows the values of the main diagonal elements of the ratio compensation matrix $\underline{\underline{R}}^{(2)}$ in (6) in p.u. of the rated ratio of the CT (dashed black line) for both fundamental magnitudes analysed.

In the x-axis the harmonic order is repeated twice because the elements of the main diagonal represent the ratios between the real:real and the imaginary:imaginary parts of primary and secondary currents of the same harmonic order, e.g. for the second harmonic: g2r2r and g2i2i.

The variation between the two operating points (~0.08%) is about one order of magnitude lower than the declared accuracy class limit.

It is also possible to observe that the values of the main diagonal elements are numerically very close to the rated ratio of the CT; a slight increase in deviation with the harmonic order is visible.

Fig. 3 shows the values of the off-diagonal elements of the compensation matrix that take into account the cross coupling existing between harmonics of different orders (cross coupling ratios) due to the non-linearities present.

It is worthwhile emphasising that the order of magnitude of such ratios is three times lower than those of the main diagonal; that is to say that the cross coupling effects of this CT are not significant in the frequency range analysed.

Figure 4 displays four spectra of the primary current, obtained in four different ways: 1) the primary current (red plus symbols) from the secondary current (average of 10 iterations) by applying the proposed compensation technique (6); 2) the primary current (blue dots) from the secondary current (average of 10 iterations) by multiplying by the rated CT ratio; 3) measured primary current (grey dots) for each of the ten iterations; 4) measured primary current (black circle symbols, average of 10 iterations).

It is possible to observe that all of the results are very close to each other, starting to slightly deviate with the harmonic order, and that during the tests the magnitude of the current slightly decreases from 10% to 9.8% due to a systematic effect of the generation system which has not been compensated.

However, the generality of the results is not affected. Fig. 5 shows the magnification of Fig. 4 around the results corresponding to the superposition of the 5-th harmonic versus its phase angle. It is possible to observe that the compensation technique adopted follows the very small sensitivity of the transducer to the phase angle of the superimposed harmonic component.

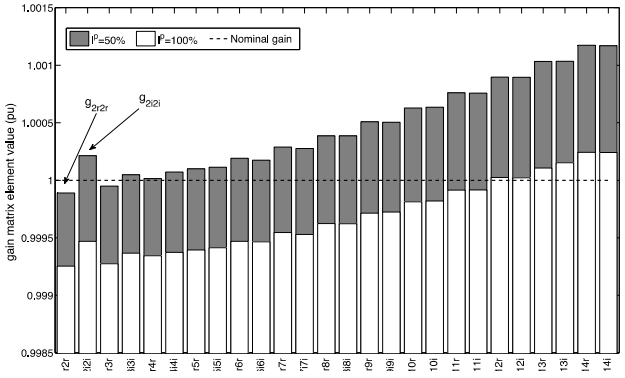

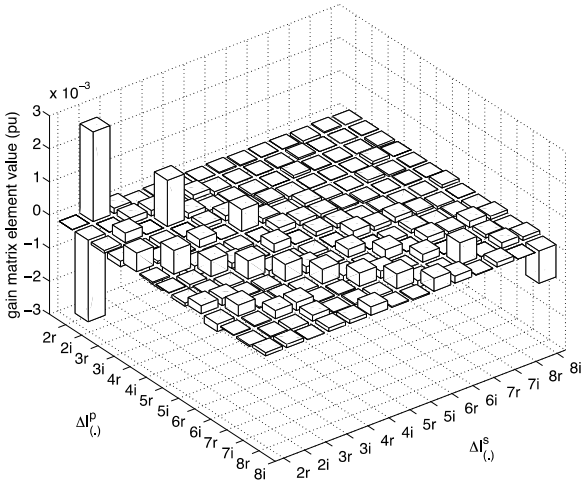

Figure 3. Values of the off-diagonal elements of the compensation matrix $\underline{\underline{R}}^{(2)}$ in (6) in pu of the rated ratio of the CT versus the harmonic order.

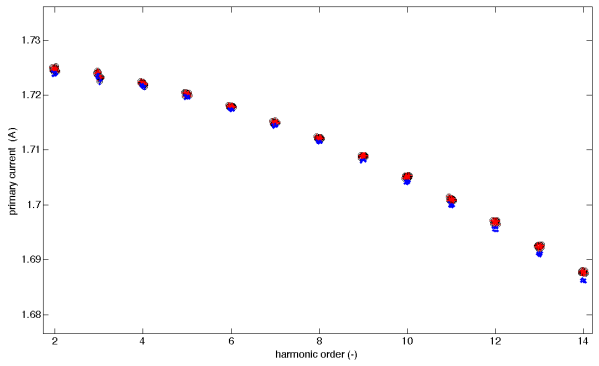

Figure 4. Spectrum of the primary current obtained using: 1) the proposed compensation technique (6) (red plus symbols); 2) measured primary current for each of the ten itartions (gray dots); 3) averaged measurements (black circle symbols); 4) the rated ratio of the CT (blue dots).

The results are also more accurate than those obtained using the constant rated ratio. Moreover, the spread of the results of the ten repetitions is very limited, as shown by the magnification of one test reported in Fig. 5.

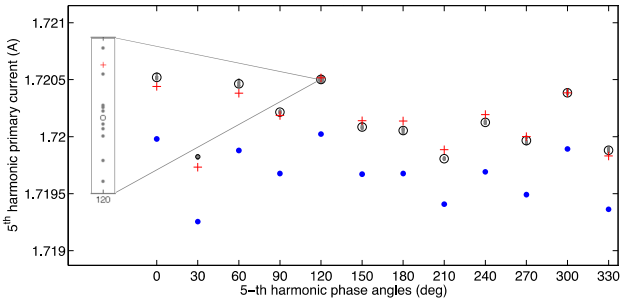

Figure 5. Zoom of Fig. 4 around the results corresponding to the superposition of the 5-th harmonic versus its phase angle.

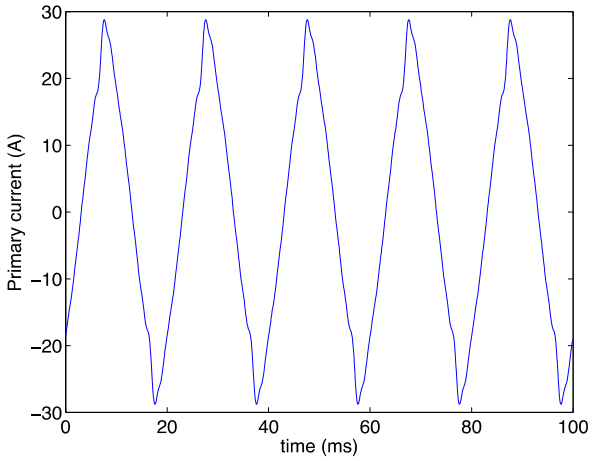

(a)

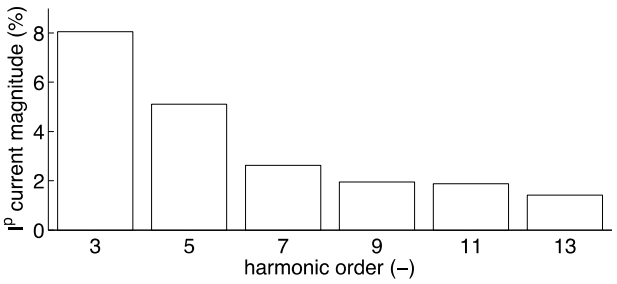

(b)

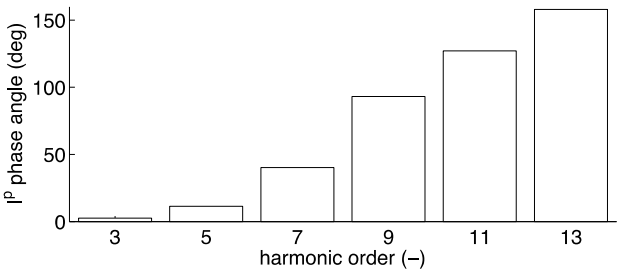

(c)

Figure 6. Generic verification signal: a) time waveform, b) and c) magnitude and phase angle versus the harmonic order.

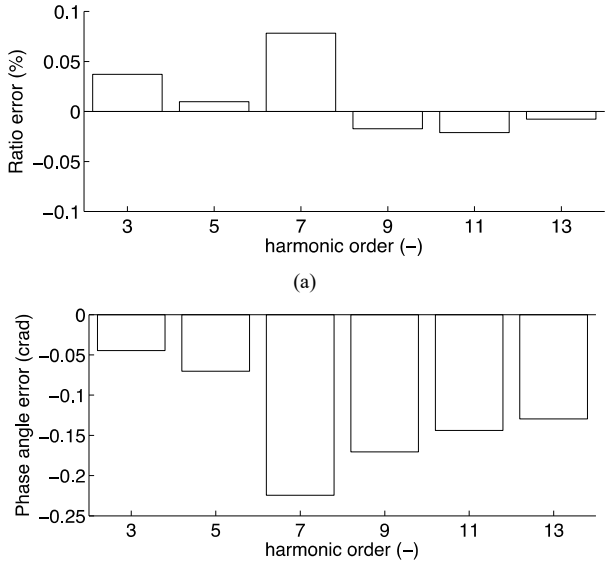

Figure 7. Ratio (a) and phase angle (b) errors obtained by the compensation techique proposed versus the harmonic order.

B. Verification by Means of a Generic Signal

Fig. 6a) shows the time domain waveform of the generic signal used for the verification, while Fig. 6b) and 6c) show the magnitude and phase angle versus the harmonic order.

Once measured, the spectrum of the secondary current has been multiplied by the compensation matrix calculated in the previous subsection.

The results in Fig. 7 show the ratio and phase errors (see (7) and (8)). It is possible to observe that the linear behaviour of the transducer is confirmed in the frequency range of interest, as both errors belong to the declared accuracy class of the CT.

V. CONCLUSIONS

In this paper, the complex ratio of the CT is modelled using a frequency domain model based on the frequency coupling matrix approach. An accurate measurement setup has been built to characterize the CTs performance in distorted conditions. Some preliminary results obtained when applying the proposed compensation technique to a Class 0.5 commercial CT have been presented and discussed.

Future work will further investigate CT performance, and the subsequent improvement afforded by the proposed compensation technique, for a wider frequency range, different burdens and more operating points. The procedure will also be applied to test other CTs with lower accuracy class.

VI. ACKNOWLEDGMENT

The paper was prepared at the SUN-EMC Lab. of the University of Campania "Luigi Vanvitelli". The authors acknowledge financial support from Italian Ministry of University and Research (Grant PON03PE-00175-1, PON03PE-00177-1, PON03PE-00178-1). The authors wish also to thank eng. Palma Sara Letizia for the help given during experimental activity.

REFERENCES

[1] G. Crotti *et al*., "Frequency Compliance of MV Voltage Sensors for Smart Grid Application," in *IEEE Sensors Journal*, vol. 17, no. 23, pp. 7621-7629, 1 Dec.1, 2017.

[2] G. Crotti, D. Giordano, M. Luiso and P. Pescetto, "Improvement of Agilent 3458A Performances in Wideband Complex Transfer Function Measurement," in *IEEE Transactions on Instrumentation and Measurement*, vol. 66, no. 6, pp. 1108-1116, June 2017.

[3] G. Crotti, D. Gallo, D. Giordano, C. Landi and M. Luiso, "A Characterized Method for the Real-Time Compensation of Power System Measurement Transducers," in *IEEE Transactions on Instrumentation and Measurement*, vol. 64, no. 6, pp. 1398-1404, June 2015.

[4] G. Acampora, C. Landi, M. Luiso and N. Pasquino, "Optimization of energy consumption in a railway traction system," *International Symposium on Power Electronics, Electrical Drives, Automation and Motion, 2006. SPEEDAM 2006.*, Taormina, 2006, pp. 1121-1126.

[5] G. Crotti, D. Gallo, D. Giordano, C. Landi and M. Luiso, "Medium Voltage Divider Coupled With an Analog Optical Transmission System," in *IEEE Transactions on Instrumentation and Measurement*, vol. 63, no. 10, pp. 2349-2357, Oct. 2014.

[6] G. Crotti, D. Gallo, D. Giordano, C. Landi, M. Luiso, "FPGA-based real time compensation method for medium voltage transducers", ACTA IMEKO, vol. Vol 4, p. 82-89, ISSN: 2221-870X, Year 2015

[7] D. Gallo, C. Landi, M. Luiso, "Severity Assessment Issues for Short Voltage Dips", *Elsevier Measurement*, Volume 43, Issue 8, October 2010, Pages 1040-1048, ISSN: 02632241

[8] D. Gallo, C. Landi, M. Luiso, E. Fiorucci, G. Bucci, F. Ciancetta, "Realization and Characterization of an Electronic Instrument Transducer for MV Networks with Fiber Optic Insulation", *WSEAS Transactions On Power Systems*, ISSN: 1790-5060, E-ISSN: 2224-350X, Issue 1, Volume 8, pages 45-56, January 2013

[9] A. Cataliotti, D. Di Cara, A. E. Emanuel and S. Nuccio, "Current transformers effects on the measurement of harmonic active power in LV and MV networks," *IEEE Trans. Power Delivery*, vol. 26, no. 1, pp. 360-368, Jan. 2011.

[10] A. Cataliotti, D. Di Cara, A. E. Emanuel and S. Nuccio, "A novel approach to current transformer characterization in the presence of harmonic distortion," *IEEE Trans. Instrumentation and Measurement*, vol. 58, no. 5, pp. 1446-1453, May 2009.

[11] M. Luiso et al., "Metrological performances of voltage and current instrument transformers in harmonics measurements", in *Proc. IEEE International Instrumentation and Measurement Technology Conference (I2MTC 2018)*, Houston, TX, USA, May, 2018, pp. 1366 – 1371.

[12] M. Faifer, C. Laurano, R. Ottoboni, S. Toscani and M. Zanoni, "Characterization of voltage instrument transformers under nonsinusoidal vonditions based on the best linear approximation," *IEEE Trans. Instrumentation and Measurement*, in press.

[13] T. Lei et al., "Behavior of voltage transformers under distorted conditions," in *Proc. IEEE International Instrumentation and Measurement Technology Conference*, Taipei, Taiwan, May, 2016, pp 1-6.

[14] N. Locci and C. Muscas, "Hysteresis and eddy currents compensation in current transformers," *IEEE Trans. Power Delivery*, vol. 16, no. 2, pp. 154-159, Apr. 2001.

[15] M. Zou, W. Sima, M. Yang, L. Li, Q. Yang and P. Sun, "Improved low-frequency transformer model based on Jiles–Atherton hysteresis theory," *IET Generation, Transmission & Distribution*, vol. 11, no. 4, pp. 915-923, 2017.

[16] X. Wang, D. W. P. Thomas, M. Sumner, J. Paul and S. H. L. Cabral, "Characteristics of Jiles–Atherton model parameters and their application to transformer inrush current simulation," *IEEE Trans. Magnetics*, vol. 44, no. 3, pp. 340-345, Mar. 2008.

[17] J. Arrillaga, B. C. Smith, N. R.Watson, and A. R.Wood, Power System Harmonic Analysis. New York: Wiley, 1997.

[18] B.C. Smith, N.R. Watson, A.R. Wood, and J. Arrillaga, "Harmonic tensor linearisation of HVDC converters," *IEEE Trans. Power Delivery*, vol. 13, no. 4, pp. 1244–1250, Oct. 1998.

[19] Y. Sun, G. Zhang, W. Xu, and J.G. Mayordomo, "A harmonically coupled admittance matrix model for AC/DC converters," *IEEE Trans. Power Systems*, vol. 22, no. 4, pp. 1574–1582, Nov. 2007.

[20] R. Carbone, A. L. Schiavo, P. Marino, and A. Testa, "Frequency coupling matrixes for multi stage conversion system analysis," *Eur. Trans. Elect. Power*, vol. 12, no. 1, pp. 17–24, Jan./Feb. 2002.

[21] Lehn P. W. Lehn and K. L. Lian, "Frequency coupling matrix of a voltagesource converter derived from piecewise linear differential equations," *IEEE Trans. Power Delivery*, vol. 22, no. 3, pp. 1603–1612, Jul. 2007.

[22] L. Frater, "Light flicker and harmonic modelling of electrical lighting," Ph.D. thesis, The University of Canterbury, Christchurch, New Zealand, 2015.

[23] L.M. Romero, L. Gallego, S. Müller and J. Meyer, "Characterization of non-linear household loads for frequency domain modeling," *Ingeniería e Investigación*, 35(Sup1), pp. 65-72, 2015.

[24] M. Fauri, "Harmonic modelling of non-linear load by means of crossed frequency admittance matrix," *IEEE Trans. Power Syst.*, vol. 12, no. 4, pp. 1632–1638, 1997.

[25] R. Langella, J. E. Caicedo, A. A. Romero, H. C. Zini, J. Meyer, and N. R. Watson, "On the use of fourier descriptors for the assessment of frequency coupling matrices of power electronic devices," in *Proc. 18th International Conference on Harmonics and Quality of Power (ICHQP)*, Ljubjana, Slovenia, May, 2018, pp. 1 – 6.

[26] J. E. Caicedo, A. A. Romero, H. C. Zini, R. Langella, J. Meyer, N. R. Watson, "Impact of reference conditions on the frequency coupling matrix of a plug-in electric vehicle charger," in *Proc. 18th International Conference on Harmonics and Quality of Power (ICHQP)*, Ljubjana, Slovenia, May, 2018, pp. 1 – 6.

[27] D. Gallo, R. Langella, M. Luiso, A. Testa and N. R. Watson, "A new test procedure to measure power electronic devices' frequency coupling admittance," *IEEE Trans. Instrumentation and Measurement*, in press.

[28] G. Crotti, D. Gallo, D. Giordano, C. Landi and M. Luiso, "Industrial comparator for smart grid sensor calibration," *IEEE Sensors Journal*, vol. 17, no. 23, pp. 7784-7793, Dec.1, 1 2017.

[29] G. Crotti, D. Gallo, D. Giordano, C. Landi, M. Luiso and M. Modarres, "Frequency response of MV voltage transformer under actual waveforms," *IEEE Trans. Instrumentation and Measurement*, vol. 66, no. 6, pp. 1146-1154, June 2017.

[30] D. Belega and D. Petri, "Accuracy analysis of the multicycle synchrophasor estimator provided by the interpolated DFT algorithm," IEEE Trans. Instrumentation and Measurement, vol. 62, no. 5, pp. 942-953, May 2013.

[31] M. Luiso, D. Macii, P. Tosato, D. Brunelli, D. Gallo and C. Landi, "A Low-Voltage Measurement Testbed for Metrological Characterization of Algorithms for Phasor Measurement Units," in *IEEE Transactions on Instrumentation and Measurement*.

[32] P. Tosato, D. Macii, M. Luiso, D. Brunelli, D. Gallo and C. Landi, "A Tuned Lightweight Estimation Algorithm for Low-Cost Phasor Measurement Units," in *IEEE Transactions on Instrumentation and Measurement*, vol. 67, no. 5, pp. 1047-1057, May 2018.